



Wind-driven water level fluctuations drive marsh edge erosion variability in microtidal coastal bays

Kendall Valentine^{a,*}, Giulio Mariotti^{a,b}

^a Department of Oceanography and Coastal Sciences, College of the Coast and Environment, Energy, Coast and Environment Building, Louisiana State University, Baton Rouge, LA 70803, United States

^b Center for Computation and Technology, Louisiana State University, Baton Rouge, LA 70803, United States

ARTICLE INFO

Keywords:

Ecogeomorphology
Soil shear strength
Waves
Coastal restoration
Louisiana
Wave overshooting
Undercut
Historical maps

ABSTRACT

Marsh shorelines are retreating rapidly in coastal Louisiana, largely driven by wind waves attacking the marsh edge. The amount of wave power hitting the marsh is a major predictor for marsh retreat rates; however, marsh erodibility (erosion rate per unit of wave power) has a large spatial variability. Identifying the causes of this variability is essential to obtain more reliable predictions and to optimize marsh protection strategies. Here we investigate marsh edge erosion in a small (~3 km²) bay within Barataria Bay, LA, USA. Long-term (~140 years) erosion data and short term (~1 year) field measurements show that, for the same wave power, north-facing marsh edges erode twice as fast as south-facing marsh edges. A possible explanation might reside in the peculiar hydrodynamics of coastal Louisiana, where northerly winds are associated with low water levels and southerly winds are associated with high water levels. This causes south-facing shores to experience high water levels when being impacted by waves and north-facing shore to experience low water levels when being impacted by waves, which could subsequently affect marsh edge erosion in three different ways. First, south-facing shores experience a higher frequency of wave overshooting, which limits the ability of waves to cause erosion. Second, north-facing shores experience a higher frequency of waves impacting the highly erodible soil below the root mat, thus undercutting the marsh. Third, south-facing marsh edges have a higher elevation and a higher soil shear strength in the root layer (0–20 cm depth), likely because these shores receive more sediment during wave events. These three processes were combined into a single empirical correction to represent effective marsh erodibility and the correction was used in a 2D model of marsh edge retreat. The model accurately predicts marsh edge erosion and can be used to determine whether historical marsh loss was due to edge erosion or to other processes, such as ponding or drowning.

1. Introduction

Approximately 25% of coastal Louisiana land area has been lost since 1930 (Couvillion et al., 2011, 2017). Rapid land loss in Louisiana has been attributed to large-scale processes of high rates of subsidence and sea level rise, as well as locally-important processes such as fluid withdrawal, building of canals and dredging, and salt water intrusion (Kolker et al., 2011; Olea and Coleman, 2014; Turner, 2014). Although the rate of land loss may have slowed over the past several years, the rate is still substantial (~28 km² y⁻¹, Couvillion et al., 2017) and poses threats to local communities and infrastructure. Identifying and quantifying the mechanisms of this loss is crucial to develop cost-effective protection and restoration activities, such as those proposed in the Louisiana Coastal Master Plan (Peyronnin et al., 2013).

Marshes erode both in the vertical direction via marsh collapse/

drowning and pond expansion (Day et al., 2011) and in the horizontal direction via marsh-edge erosion (Leonardi and Fagherazzi, 2014). On the large scale, this latter process is primarily attributed to wind-waves, which impact the marsh edge and leads to both a gradual surface erosion as well as the detachment of entire blocks (Schwimmer, 2001; Marani et al., 2011; Bendoni et al., 2016; Wang et al., 2017), and eventually leads to erosion rates ranging from 0.1 to 10 m yr⁻¹ (Schwimmer, 2001, Leonardi et al., 2016). Tidal currents (Gabet, 1998), soil creep (Mariotti et al., 2016), and biological processes such as crab burrowing (Raposa et al., 2018) might also cause marsh edge erosion, even though these processes tend to be relegated to channel banks and are generally associated with slower retreat rates (0.1–0.5 m yr⁻¹) (Ensign et al., 2017; Smith, 2009; Hartig et al., 2002; Mariotti, 2018).

Marsh edge retreat has been linearly related to wave power (Marani

* Corresponding author.

E-mail address: kvalen7@lsu.edu (K. Valentine).

<https://doi.org/10.1016/j.csr.2019.03.002>

Received 29 August 2018; Received in revised form 22 February 2019; Accepted 5 March 2019

Available online 06 March 2019

0278-4343/ © 2019 Elsevier Ltd. All rights reserved.

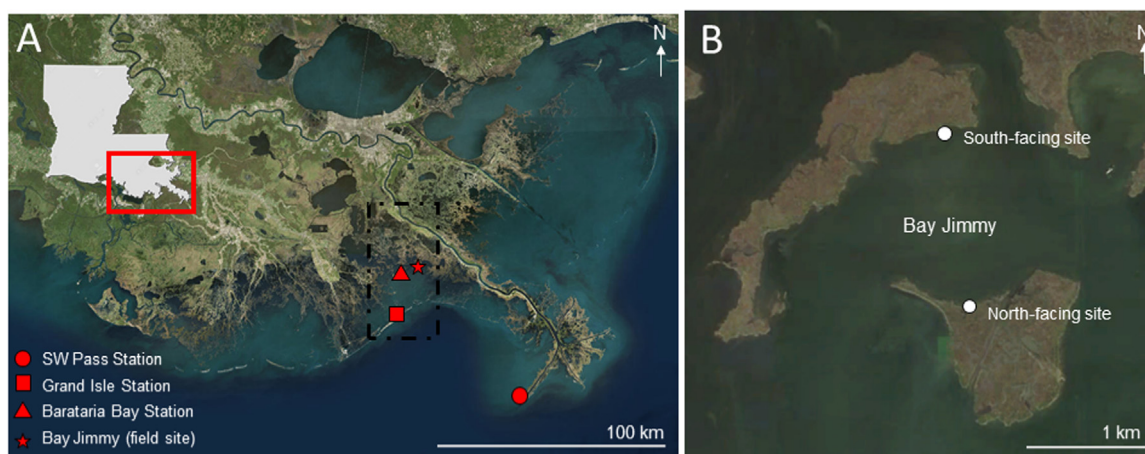


Fig. 1. (A) Figure of the state of Louisiana and map of coastal Louisiana (Landsat, Google Earth). Red box over the state outline indicates the extent of area shown and red triangle, circle, and square indicate locations of wind and water level measurements. The star designates location of field work. The black dashed-line indicates the model domain. (B) Map of Bay Jimmy, a sub-bay of Barataria Bay. Markers indicate location of wave sensors. Image (Landsat) downloaded from Google Earth (November 2016).

et al., 2011; Leonardi et al., 2016) in both micro- and meso-tidal systems, further supporting the dominance of wind-waves as a driver of marsh edge erosion. Locally, marsh edge erosion rates can be dictated by sediment composition, vegetation properties (Feagin et al., 2009; Wang et al., 2017), and benthic invertebrate communities (i.e. crab burrows, mussel colonies) (Bertness, 1984; Escapa et al., 2007; Hughes et al., 2009; McLoughlin, 2010). Despite recent progress, there still are large uncertainties on how marsh edge erosion takes place and what causes its spatial variability.

For micro- to meso- tidal systems, the rate at which marsh edge erosion takes place strongly depends on the power of the locally generated waves (Schwimmer, 2001; Leonardi et al., 2016), which increases monotonically with wind speed, fetch, and water level (Young and Verhagen, 1996; Fagherazzi and Wiberg, 2009). As such, increases in water level within shallow tidal basins – for example during storm surges – cause an increase in wave power and consequently should also increase marsh edge erosion. In basins with large asymmetric water level variations due to wind patterns, marshes with different orientations with respect to the wind direction are thus expected to erode at different rates (Mariotti et al., 2010).

While water level can influence wave power, it also affects the erosion of the marsh edge by altering the wave thrust that impacts the marsh. Wave thrust increases with water level up until the marsh platform is submerged; once the water level is higher than the marsh the wave thrust rapidly decreases because part of the wave “overshoots” the marsh (Tonelli et al., 2010). Overshooting waves are subsequently attenuated over the vegetated marsh platform, thus not causing further erosion (Moller et al., 2014; Moller and Spencer, 2002). As such, the process of wave overshooting is expected to reduce the ability of waves to erode the marsh edge.

In addition to wave characteristics, the rate of marsh edge retreat strongly depends on marsh erodibility. This parameter is a complex function of soil properties, which can be highly variable within a given marsh, thus suggesting marsh erodibility to be highly variable as well. Indeed, field measurements indicate that marsh sites with different characteristics erode at different rates even if subjected to the same wave power (Priestas et al., 2015). State-of-the-art marsh evolution models, however, often keep erodibility as a constant calibration parameter (Mariotti and Fagherazzi, 2010; Mariotti and Canestrelli, 2017), with the implicit assumption that soil properties are spatially uniform.

Plant roots are able to reduce erosion by stabilizing sediments (Le Hir et al., 2007; Turner, 2011), suggesting that root strength might affect the overall marsh edge erodibility. Additionally, plant shoots help

trap mineral sediment, thus promoting vertical accretion and increasing marsh elevation (Le Hir et al., 2007). Marsh elevation, in turn, controls the hydroperiod and thus affects the plant species assemblages (Silvestri et al., 2005). Since different plants have different root strengths (Hollis and Turner, 2018), species zonation might create heterogeneities in root strength and therefore marsh erodibility. In Louisiana, variations in marsh erodibility are also closely linked to the distribution of oil from spills, such as the Deepwater Horizons spill in 2010 (McClenachan et al., 2013). Oil from the Deepwater Horizons spill was dispersed nonuniformly across Barataria Bay, impacting some marsh edges more than others (Nixon et al., 2016) and thus increasing spatial variability in erosion rates (Rangoonwala et al., 2016).

Water level might also have compounding effect with the vertical distribution of marsh strength. Roots only provide strength in the top layer (~20 cm) but not in the underlying layers, a gradient that is often manifested by the presence of undercutting at the base of the marsh and overhanging at its top (Schwimmer, 2001; Turner, 2011; Francalanci et al., 2013; Hollis and Turner, 2018). In Louisiana marshes, a twofold difference in soil strength between the root layer and the underlying sediment has been measured (11 kPa in root layer vs. 5 kPa beneath roots, Turner, 2011). As such, waves hitting when the water level is below the root zone might be more effective at eroding the marsh than waves hitting when the water level is at the root zone.

The purpose of this study is to determine how wind-driven water level changes affect marsh edge erosion in coastal microtidal bays. We hypothesize that water level changes related to wind direction alter overshooting, undercutting, and vertical accretion at the marsh edge, causing heterogeneous erosion within a given marsh. These processes were combined into a single empirical correction to represent effective marsh erodibility and the correction was used in a 2D model of marsh edge retreat.

2. Methods

2.1. Study site

Barataria Bay (Fig. 1A), a shallow, semi-protected interdistributary bay, is representative of much of the Louisiana coast. Marsh sediments in lower Barataria Bay are primarily composed of mud (80–90% of inorganic fraction silt + clay), have 20–35% organic matter by weight, and have an average bulk density of 0.2–0.3 g cm⁻³ (Wilson and Allison, 2008; DeLaune and White, 2012; Pietroski et al., 2015). Astronomic tides are microtidal (0.3 m), but larger water level variations can be caused by wind. Previous studies have shown that along the northern

Gulf of Mexico coast, southerly winds are correlated with higher water levels and northerly winds are correlated with lower water levels (Kemp et al., 1980; Hsu, 1988; Feng and Li, 2010). Southeasterly winds dominate for much of the year but are interrupted by northerly winds with the passage of cold fronts during October – April (Dimego et al., 1976; Roberts et al., 1987).

2.2. Historical data

Wind speed and direction data from 1990 to 2017 were downloaded from NOAA for the sensor at Southwest Pass (NDBC, Station BURL1) and from 2016 to 2017 for Barataria Bay (USGS, Station 07380251) (Fig. 1). Wind speed and direction, measured every six minutes, were averaged for each hour. The Southwest Pass wind data were used because the time series is longer, while Barataria Bay wind data were also used because the station was closer to the study area (Fig. 1A). Winds from Southwest Pass, measured at 38 m above mean sea level, were corrected to the standard 10 m height; winds were measured at a height of 10 m at the Barataria Bay site and did not need this correction. Corrected winds from Barataria Bay and Southwest Pass were statistically similar (Mariotti et al., 2018), suggesting that they could be both used as a proxy for the wind in Barataria Bay.

Water level data were downloaded from Grand Isle, LA from 1990 to 2017 (NOAA Tides and Currents, Station 876174). Next, we used GIS analysis to calculate centennial scale marsh loss in lower Barataria Bay, from the barrier islands to the brackish zone. Historical shoreline surveys from 1877 (NOAA T-Sheets T01468BA and T01468B) were re-sampled over a grid with 30 m resolution. The absence of misalignment in the historical maps was confirmed by noticing that – at the 30 m resolution scale – the position of the tidal channels did not vary considerably between 1877 and present time. Landsat-8 images with 30 m resolution were used to calculate the land-water extent in 2016. Following a previous study of marsh edge erosion in Barataria Bay (Rangoonwala et al., 2016), we used a simple threshold to separate images into marsh and open water classes. By looking at satellite images with higher resolution (0.5–1 m), we estimated that the error due to different water levels is generally on the order of a few meters, and up to 10 m in presence of complex features (e.g., sheared vegetation) at marsh edge. Even considering the latter case, the error associated with marsh edge geometry and variable water levels is smaller than the error associated with the pixel size. Therefore, both the historical and the modern maps have an estimated error of 30 m. This error is generally much smaller than the typical erosion during the 139-year span, which is on the order of 1 km. Furthermore, the successful application of 30 m resolution Landsat images to estimate marsh erosion by ponding in the Mississippi Delta over a much shorter (34 years) time span (Ortiz et al., 2017) supports the robustness of our analysis. The maps included lower Barataria Bay, from the barrier islands to brackish area. Maps of marsh salinity by plant type (marine, brackish, intermediate, fresh) for years 1949, 1968, 1978, 1988, 1997, 2001, 2007, and 2013 were downloaded from Louisiana's Coastwide Reference Monitoring System (CRMS).

2.3. Field sampling and analysis

We focused the study on Bay Jimmy, a sub-bay of the larger Barataria Bay (Fig. 1B). Within this bay we considered two sites: a south-facing shore and a north-facing shore. The two sites had similar fetches (1.5 km) when either northerly or southerly winds blew.

Four RBR Ltd. sensors were deployed in Bay Jimmy for one year and measured pressure at 4 Hz in 1024-point bursts (approximately 5 min) once an hour. At both the north- and south-facing shores, we deployed two sensors: one offshore 10 m from the marsh edge and one on the marsh platform 3 m from the marsh edge. We surveyed the sites with an RTK-GPS (Leica GS14 GNSS). We used a shear vane (Humboldt H-4227) to measure the shear strength profiles of the soils every 10 cm down to

50 cm in depth. These measurements were taken 50 cm from the marsh edge, in five replicate profiles at each site. PVC poles were placed 3 m from the marsh edge and the distance between the poles and the edge was measured to calculate the short-term edge erosion rate.

The pressure spectrum was created using a fast Fourier transform of the collected pressure data and was converted to the surface elevation spectrum using linear wave theory (Tucker and Pitt, 2001). A frequency-dependent correction was applied to the pressure to account for depth attenuation. Significant wave height and peak period were determined using the calculated spectra.

2.4. Model design

A simple 2D model of marsh edge retreat for wind waves was used to predict coastline change in Barataria Bay, LA. Within the model domain, each cell was defined as either marsh or open water (mudflat). For each time step (one year), a random wind speed and direction were selected from the wind distribution from Southwest Pass. The random selection from the wind time series allows us to consider rare events with strong winds (maximum wind on record: 29 ms^{-1}). The fetch was calculated for each boundary cell (a marsh cell surrounded by at least one open water cell) using a geometric model, which calculated the length of open water in front of the marsh edge for a given wind direction. Wave properties were calculated using semi-empirical relationships that related significant wave height (H_s) and wave period (T_p) to wind speed, water depth, and fetch (Young and Verhagen, 1996). The depth of the open water was set equal to 0.8 m to represent the depth ~10–20 m from the marsh edge (1.0 m from Wilson and Allison, 2008, 0.6 m measured in this study). The model is highly simplified and has a uniform depth across the domain. As this model does not include wave propagation and instead relies upon an empirical relationship between wind speed, fetch, and the local depth, we assume that the waves instantaneously adjust to the local water depth. Indeed, only the waves near the marsh edge (i.e. those at depths 0.6–1 m) affect marsh edge erosion and thus the locally calculated waves based on the instantaneous wind speed, fetch and a depth of 0.8 m would reasonably represent the waves.

We calculated the wave power at each boundary cell from the wave height and period according to

$$P = \frac{1}{16} \rho g H_s^2 c_g \quad (1)$$

where c_g is the group wave velocity, which is determined from the peak period and water depth, ρ is the water density, and g is the gravitational constant. For each edge cell, the total wave power impacting the edge was calculated as the sum of the wave power in all adjacent cells. We assumed that the edge erosion rate was linearly proportional to the wave power (Marani et al., 2011; Leonardi et al., 2016),

$$E = \alpha P \quad (2)$$

where α is an erodibility coefficient. We then used a probabilistic method for eroding the boundary cells (Mariotti and Canestrelli, 2017). For a given cell, the probability of erosion (P_E) of the cell during the time interval Δt depends on the calculated erosion E and the cell size (Δx):

$$P_E = \frac{E \Delta t}{\Delta x} \quad (3)$$

The implementation of the erosion probability into the cellular-automata model is straightforward: a random number is taken from a uniform distribution between 0 and 1 and if the random value is less than P_E , the entire cell is eroded and becomes open water, otherwise the cell is not eroded. According to this method, the expected value for the erosion rate coincides with the deterministic erosion rate E ; as such, long-term simulations (in which the probabilistic erosion procedure is repeated many times) converge to the deterministic method.

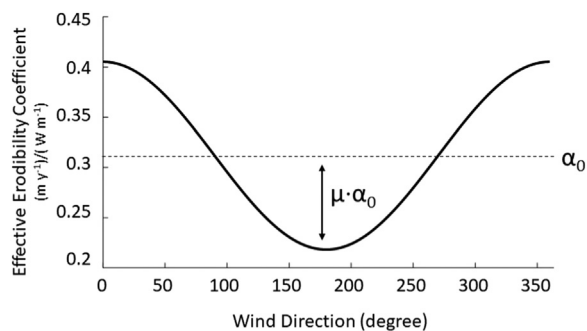


Fig. 2. Direction-dependent effective erodibility incorporated into the model of marsh edge erosion. The erodibility coefficient depends on wind direction, which serves as a proxy for the orientation of the shoreline.

The model was initialized based on the 1877 map, using the same 30 by 30 m cell resolution. The model was run over an area of 50 km by 30 km, comprising lower Barataria Bay (Fig. 1A); however, the model was calibrated to Bay Jimmy because we had field measurements in this bay. For the basic (isotropic) version of the model, we calibrated the model using a constant α value for the erodibility coefficient to achieve the best fit between the model and measured marsh change. To improve the model performance, an anisotropic version of this simple model was created by introducing a direction-dependent empirical correction. The erodibility coefficient is described as:

$$\alpha = \alpha_0 (1 + \mu \cos(\theta)) \quad (4)$$

where α_0 is the background erodibility coefficient, μ is the amplitude of the variability of α around α_0 , and θ is the wind direction, with zero being northerly winds. In this model version, the erodibility increased during northerly winds and decreased during southerly winds (Fig. 2).

2.5. Model performance and statistical methods

The intersection divided by the union of the erosion matrices was used to quantitatively compare the performance of each model and calibration parameters according to:

$$\Pi = (X_{\text{model}} \cap X_{\text{measured}}) / (X_{\text{model}} \cup X_{\text{measured}}) \quad (5)$$

where X_{model} are the marsh cells eroded in the model simulations and X_{measured} are the marsh cells that actually eroded according to the GIS analysis. This metric incorporates both the amount of erosion and the overlap between predicted and measured erosion. This metric ranges from zero to one; the closer this value is to one, the more similar the model and reality are.

Statistical analysis comparing measured northerly and southerly wind speeds utilized a two-sample Kolmogorov-Smirnov test (K-S test). P-values less than 0.05 were considered significant.

3. Results

3.1. Historical data

3.1.1. Historical wind and water level

Winds recorded at the Southwest Pass station typically blew from the north or from the southeast with similar frequency and magnitude (Fig. 3A). Northerly winds (300–60°) blew on average $5.1 \pm 2.4 \text{ ms}^{-1}$; southerly winds (120–240°) blew on average $4.7 \pm 2.7 \text{ ms}^{-1}$. Northerly winds were significantly stronger than southeasterly winds over the 28-year period (K-S test, $p < 0.001$). Southerly winds blew more frequently (41% of the time) compared to northerly winds (38% of the time).

Wind direction, wind speed, and water level in coastal Louisiana showed a clear relationship (Fig. 4); water level was higher on average when winds blew from the south and lower on average when winds

blew from the north. This change in water level with wind direction was amplified with increased wind speed.

3.1.2. Waves – observed vs. modeled

Winds from the Barataria Bay station were used to calculate wave properties within Bay Jimmy using semi-empirical equations (Young and Verhagen, 1996). For this comparison, only the waves measured ten meters in front of the marsh were considered. The calculated wave heights agreed well with the measured wave heights (Fig. 5). At the south-facing site during southerly winds, the measured and calculated H_s values showed no bias and agreed well with each other (slope = 1.05, $R^2 = 0.44$, Fig. 5B). At the north-facing site, the model slightly overestimated the measured waves (slope = 1.35, $R^2 = 0.58$, Fig. 5D). Lower water levels at the north-facing site could have contributed to smaller measured wave heights, whereas the model did not account for the slight changes in water level and would therefore overestimate wave heights.

After verifying the use of the semi-empirical equations, we applied these relationships to the 30-year time-series of wind from Southwest Pass to explore the long-term behavior of the Bay. The predicted cumulative wave power (30 years) associated with the incident waves from the south (120–240 degrees, $720 \text{ kJ m}^{-1} \text{ s}^{-1}$) was 29% higher than the cumulative wave power from the waves from the north (300–60 degrees, $560 \text{ kJ m}^{-1} \text{ s}^{-1}$; Fig. 3B). The measured cumulative wave power (one year) from the south ($36 \text{ kJ m}^{-1} \text{ s}^{-1}$) was 71% higher than the cumulative wave power from the north ($21 \text{ kJ m}^{-1} \text{ s}^{-1}$) (Fig. 3C). The wave power, both modeled (Fig. 3B) and measured (Fig. 3C), demonstrated that most wave power came from either the north or the south, with slightly more wave power coming from the south.

3.2. Field measurements

3.2.1. Wave parameters

The north- and south-facing sites within Bay Jimmy experienced similar wave climates (same fetch, similar wind exposure, similar wave power, Figs. 3 and 4), but the marsh edges retreated at different rates. This GIS analysis indicated that the north-facing site eroded at a rate of 1.3 m yr^{-1} over the period 1877–2013, while the south-facing site eroded at a rate of 0.5 m yr^{-1} over the same period. During the field measurement period (2016–2018), the north-facing site eroded at a rate of 1.2 m yr^{-1} and the south-facing site eroded at a rate of 0.68 m yr^{-1} based on erosion pin measurements.

At the south-facing site, the water level in front of the marsh varied from a minimum of 0.05 m to a maximum of 1.52 m above the bay bottom, with a mean depth of $0.84 \pm 0.18 \text{ m}$ (Fig. 6B–D). The first half of the time-series (May–November 2016) was characterized by regular spring-neap tidal cycles. The second half of the time-series showed irregular changes in water level, likely associated with wind induced processes. The corresponding on-land sensor was submerged approximately 31% of the time. The average depth of inundation was $0.07 \pm 0.09 \text{ m}$, with a maximum of 0.57 m. At the north-facing site, the water level at the sensor in front of the marsh varied from 0 to 1.48 m above the bay bottom, with a mean depth of $0.64 \pm 0.30 \text{ m}$ ten meters offshore (Fig. 6E–G). Similar to the data from the south-facing site, the first half of the data (May–November 2016) at the north-facing site were characterized by regular spring-neap tidal cycles while the second half of the time series recorded irregular changes in water level. The average inundation depth on the marsh platform was $0.02 \pm 0.06 \text{ m}$, with a maximum of 0.54 m. The platform was submerged 46% of the time during the deployment.

At the south-facing site, waves in front of the marsh reached heights of 0.38 m, with an average of $0.07 \pm 0.06 \text{ m}$; during inundation, waves on the marsh platform were as high as 0.30 m and averaged $0.01 \pm 0.03 \text{ m}$. At the north-facing site, waves in front of the marsh reached heights of 0.28 m and had an average of $0.03 \pm 0.03 \text{ m}$; the maximum wave height on the marsh during inundation was 0.11 m and

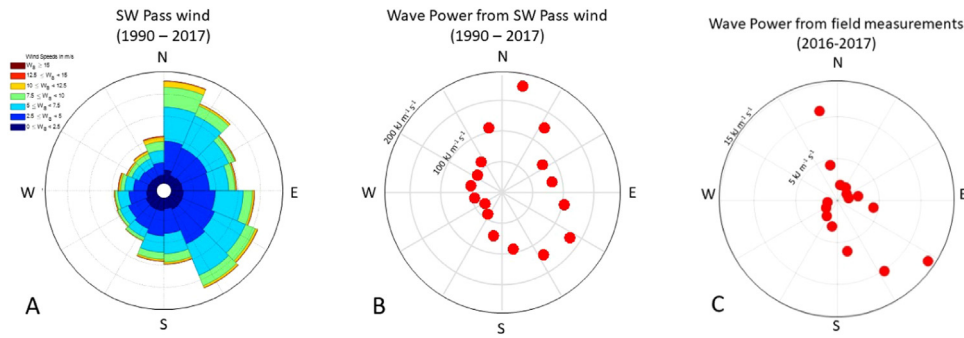


Fig. 3. (A) Wind rose for Southwest Pass 1990–2017, (B) calculated cumulative wave power based on Southwest Pass wind and semi-empirical equations, and (C) cumulative wave power calculated from measured wave characteristics in Bay Jimmy.

the average wave height was 0.01 ± 0.01 m. At both sites, wave periods were small (~ 2 s), indicative of wind-waves and few to no swell waves.

3.2.2. Waves and the marsh edge

Next, waves were analyzed in relation to the water level and the marsh edge geometry. When water level is high compared to the marsh platform, waves overshoot and contribute less to edge erosion (Tonelli et al., 2010). Additionally, when water level is below the stabilizing roots, the edge is more erodible and leads to undercutting of the root mat. Overshooting was defined as when the water level was above the elevation of the marsh platform, the root mat was defined as the top 20 cm of the marsh soils, and water levels more than 20 cm below the marsh platform were considered to be undercutting.

Approximately 35.7% of the wave power at the south-facing site overshoot the marsh platform; at the north-facing site, 18.2% of the wave power overshoot the marsh platform (Fig. 7A). A total of 30.6% of the total wave power at the south-facing site undercut the marsh platform (less than -0.20 m elevation compared to the marsh platform); 62.5% of the total wave power contributed to undercutting at the north-facing site. The width of the root mat was small (20 cm), but 33.7% of the total wave power impacted the marsh edge when water levels were at root mat height at the south-facing site and 19.2% of the total wave power at the north-facing site impacted the root mat.

3.2.3. Field site survey

Both the north and south sides of Bay Jimmy displayed typical marsh profiles (Fig. 8C), consisting of a marsh platform, marsh edge, and bay bottom (Wilson and Allison, 2008). The marsh platform at the south-facing site had an elevation of 0.29 ± 0.04 m (NAVD 88); the

north-facing site marsh platform elevation was 0.22 ± 0.04 m (NAVD 88).

At both sites the marsh soil had higher shear strength in the surface layer than in the lower layers (Fig. 7B). Within the root layer, however, the shear strength was higher at the south-facing site than at the north-facing site. Both sites achieved a similar shear strength at 0.25 m depth and continued to remain similar with increasing depth.

3.3. Marsh edge evolution model

Model results were compared to the measured land loss in Barataria Bay (Fig. 8A). The best fit with the isotropic model was obtained using an erodibility coefficient of $0.312 \text{ (m yr}^{-1})/(\text{W m}^{-1})$. This model predicted similar erosion for both the south- and north-facing sites in the microbays within Barataria Bay (Fig. 8B). As such, the model overestimated the erosion on the south-facing shore of Bay Jimmy and underestimated the erosion on the north-facing shore.

The anisotropic model reproduced the asymmetry between erosion rates at the north and south shores (Fig. 8C). The best fit was obtained using a background erodibility of $0.305 \text{ (m yr}^{-1})/(\text{W m}^{-1})$ and an amplitude of the direction-dependent correlation, μ , of 0.3 (Fig. 2, Eq. (5)). This calibration, when applied to the entirety of the model domain (lower Barataria Bay), reproduced the asymmetry in north- and south-shoreline erosion in other microbays (Fig. 9A-B, D). The model performed $\sim 8\%$ better in Bay Jimmy, and overall did a better job ($\sim 4\%$ better) in predicting erosion in areas dominated by microbays (Fig. 10). Both the isotropic model and the anisotropic model performed poorly in the northern and western regions of the domain (Figs. 9C and 12).

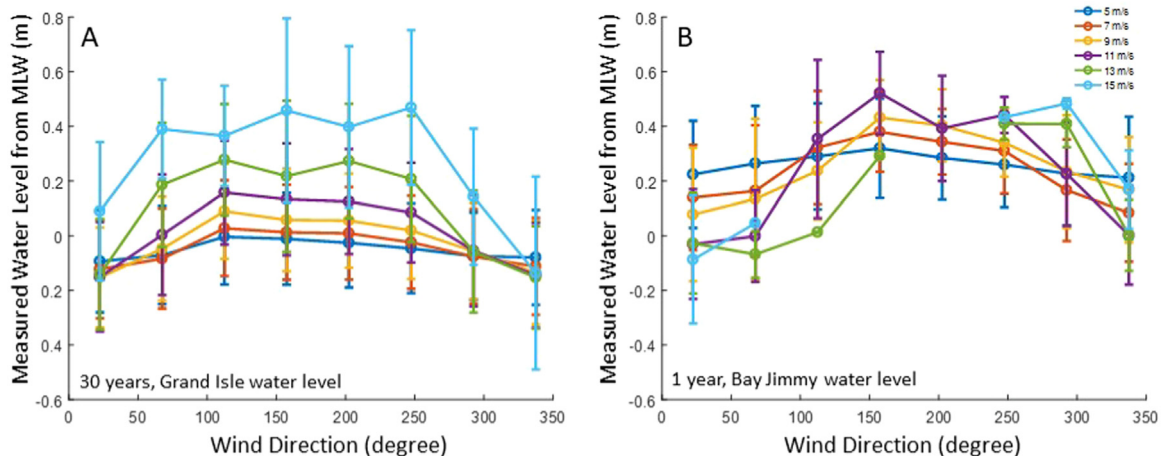


Fig. 4. Measured water level relative to mean low water (MLW) measured at Grand Isle (A) and Bay Jimmy (B) compared to wind direction. Colors represent different wind speeds.

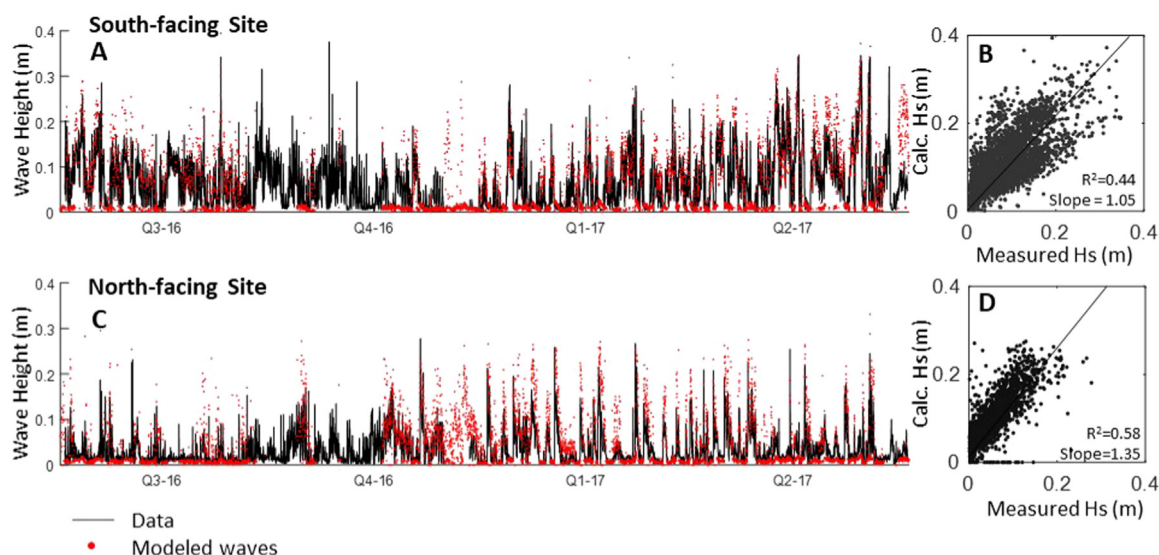


Fig. 5. Measured wave heights compared to calculated wave heights at both the south- (A, B) and north-facing (C, D) sites in Bay Jimmy.

4. Discussion

4.1. Asymmetry in Erosion

The relationship between wind and water level within Barataria Bay (Fig. 4) is consistent with previous findings of water level changes in bays on the Gulf Coast (Murray, 1976; Wax, 1977; Kemp et al., 1980; Reed, 1989; Perez et al., 2000). Northerly winds push water out of the bays and therefore lower water level; southerly winds push water into the bays from the Gulf and increase water level. Neither easterly nor westerly winds alter water level, as they do not drive water in or out of Barataria Bay. The wind-driven water level changes have been implicated in many coastal processes, such as sediment fluxes (Perez et al., 2000), and we postulate that, all else being equal, this difference in water level leads to the asymmetric erosion of north- and south-facing shorelines.

A previous model (Mariotti et al., 2010) suggested that water level differences drive asymmetries in marsh edge erosion by affecting the wave power, which increases monotonically with the water depth. Given the water level patterns in coastal Louisiana, the model of Mariotti et al. (2010) would predict the south-facing site to receive larger wave power and thus erode faster. The measurements do indeed show that the south-facing site experiences slightly larger wave powers, partly associated with the higher water levels and partly associated with the preponderance of strong winds from the south-east. This model prediction is however in striking contrast with the observation that the north-facing site is eroding twice as fast as the south-facing site (Fig. 8A). Our explanation is that the predictions of Mariotti et al. (2010) focused on extreme events that are associated with large (> 0.5 m) changes in water levels. Recent studies suggest instead that most of the marsh edge erosion is associated with moderate wind events (Leonardi et al., 2016), which generally brings water level variations of 0.1–0.3 m (Fig. 4). These water level variations are not large enough to create large asymmetries in wave power (Fig. 3), but we suggest that they can affect three processes that are sensitive to small water level variations: wave overshooting, wave undercutting, and variability in marsh strength. These three processes occur in concert, all potentially driving the south-facing shorelines to erode slower compared to north-facing shorelines.

4.1.1. Wave overshooting

Previous studies have shown that, for a given incident wave height at the marsh edge, the wave thrust against the marsh edge decreases as

water levels increasingly exceed the elevation of the marsh platform (Tonelli et al., 2010). Intuitively, these high water levels allow for overshooting; waves do not completely dissipate at the edge but rather transmit some of their energy over the marsh platform. Since this “overshot” energy over the marsh platform is eventually dissipated by the friction from the bed and from the vegetation (Moller and Spencer, 2002), it is plausible to assume that this energy does not contribute to the mechanisms of marsh edge erosion.

In order to quantify the occurrence of overshooting at the two sites, we calculated the amount of overshooting (defined as the ratio between the wave height on the marsh and the wave height in front of the marsh) as a function of the water depth over the marsh platform. As intuitively expected, at both sites the amount of overshooting increases with the water depth over the marsh (Fig. 11). An asymmetry between the two sites is present because of the correlation between wind (and thus wave) direction and water levels; 36% of the incoming wave power at the south-facing site occurred when the water level exceeded the marsh elevation, whereas only 18% of the incoming wave power at the north-facing site occurred when the water level exceeded the marsh elevation (Fig. 7A). Consequently, more wave energy should have overshoot at the south-facing site than at the north-facing site. We therefore conclude that despite both sites experiencing a similar amount of incoming wave power at the marsh edge (Fig. 3), a larger fraction of the wave power did not contribute to marsh edge erosion at the south-facing site, thus providing an explanation for the slower retreat rate.

4.1.2. Wave undercutting

Another explanation for the difference in erosion between north- and south-facing shorelines is related to the vertical gradient in marsh strength. At both sites, the upper 20 cm of the marsh edge have a greater soil shear strength compared to the lower layers (Fig. 7B). This transition coincides with the depth of the root layer, supporting previous findings that soil shear strength in salt marshes is correlated to belowground biomass, particularly larger roots and rhizomes (Scheepers, 2017).

Many studies have suggested that below-ground biomass (roots and rhizomes) increase sediment stability in marshes (Chen et al., 2012; Francalanci et al., 2013; Wang et al., 2017; Hollis and Turner, 2018). The vertical difference in soil strength can result in cantilevered marsh edge profiles, which subsequently contribute to mass failures and increase lateral erosion rates (Bendoni et al., 2016). A flume study found that at a small scale, plants can actually enhance particle erosion within

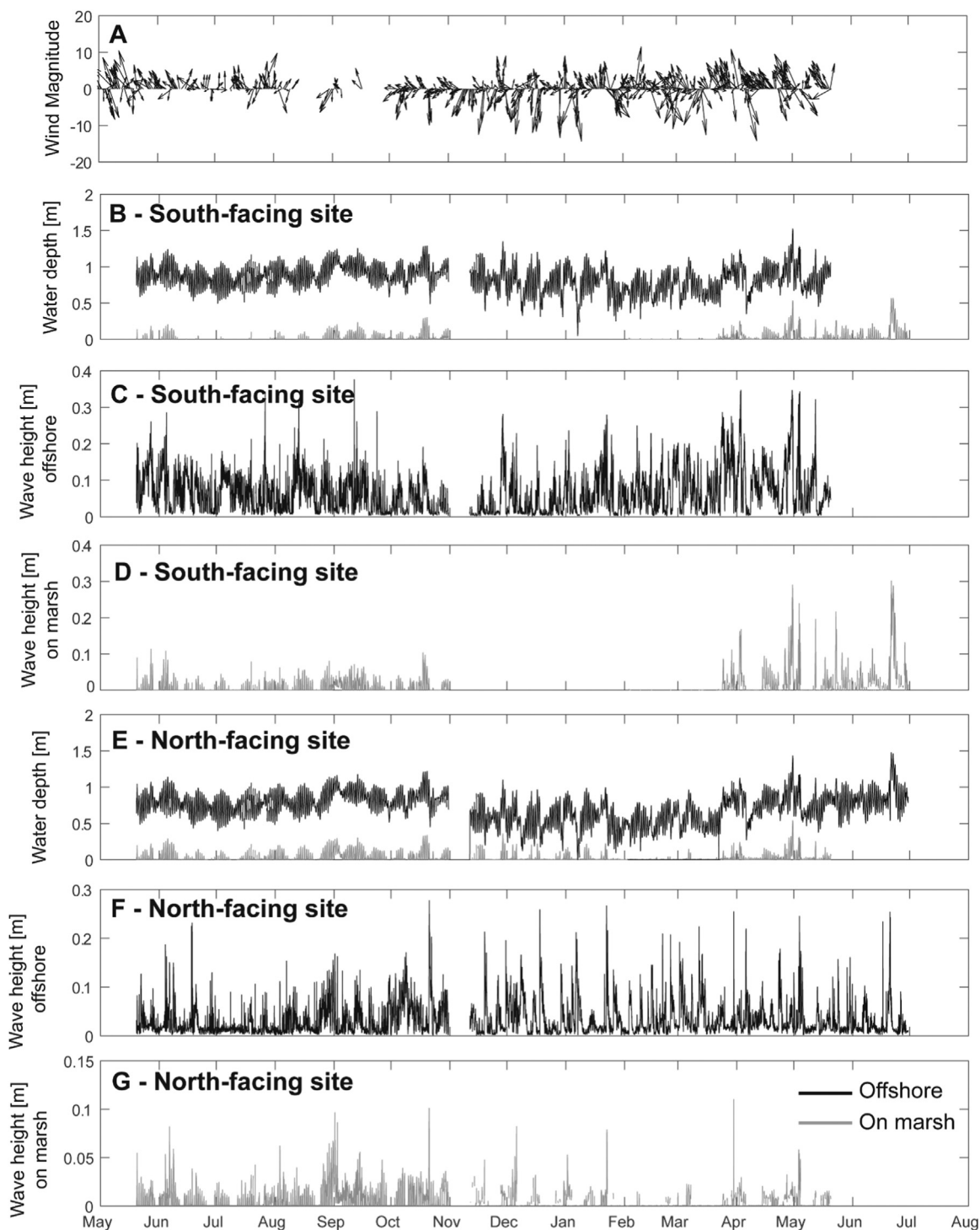


Fig. 6. (A) Wind direction and speed from the Barataria Bay wind station. South-facing site water level (B) and wave height (C and D). North-facing site water level (E) and wave height (F and G). 10 m offshore data are in black; data from the marsh platform are in grey. Note data gap for sensor on marsh from November-April for the south-facing site.

the root mat (Feagin et al., 2009). On a larger scale, however, even if sediment particles erode from the root matrix, the root mat remains. While this root mat becomes increasingly weaker from the particle erosion described by Feagin et al. (2009), a densely packed root mat would create the commonly-observed cantilever profile. Indeed, continued wave action would weaken this marsh edge and lead to a mass failure of the root mat, contributing to lateral erosion.

Based on the measured shear strength of the soils and the wave-water level distribution, we can provide a possible explanation for the

asymmetry in erosion between north- and south-facing shores. The north-facing shore is impacted by waves during northerly winds (and therefore during periods of lower water level), which erode the marsh edge below the plant roots and lead to high retreat rates (Fig. 7A). The south-facing shore is attacked by waves during southerly winds (higher water level) and therefore the waves impact the relatively strong root mat leading to less erosion. Even though the wave power associated with northerly and southerly winds are similar (Fig. 3), the location of wave impact on the marsh edge alters the erodibility of the marsh.

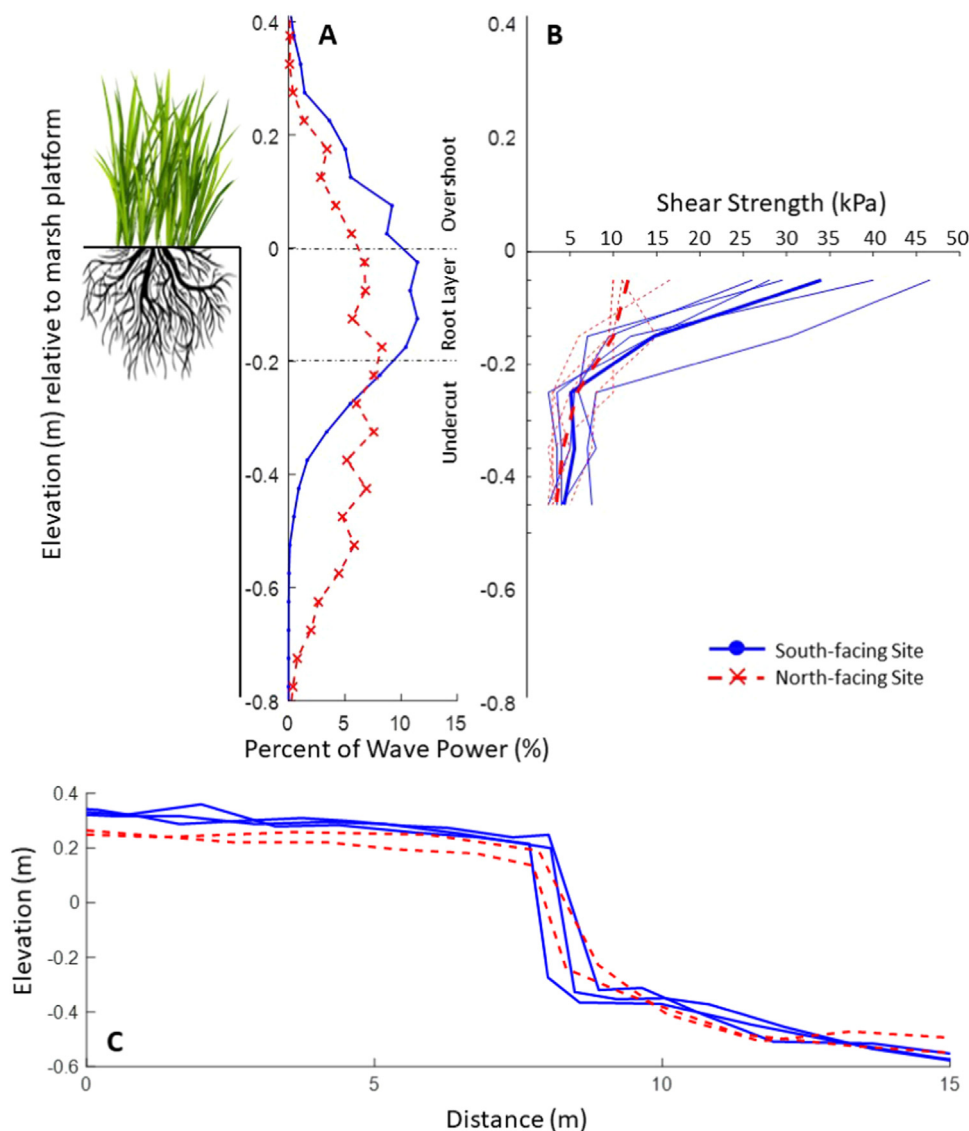


Fig. 7. (A) Percent of wave power impacting the different elevations of the marsh edge at the south-facing (blue) and north-facing (red) sites relative to the marsh platform elevation. (B) Profiles of shear strength (kPa) with depth for the south- and north-facing sites in Bay Jimmy, LA. Bolded lines indicate the average profiles for each site and thin lines indicate each profile. Depth is relative to the local marsh surface. (C) Elevation profiles from the south-facing (blue solid line) and north-facing (red dashed line) site.

4.1.3. Inter-site variability in marsh strength

Inter-site differences in marsh soil strength could also explain the spatial variability in marsh edge erosion. Spatial variations in soil properties are often invoked when comparing marshes from different settings, for example marshes located behind a barrier island as opposed to adjacent to the mainland (Prietas et al., 2015), but are generally not considered within a single marsh with seemingly uniform setting. Here we suggest that variability in marsh strength could be present at small scales (a few kilometers), through a mechanism that is tied to the patterns of wind-driven water levels.

The south-facing marsh platform is 0.05 – 0.1 m higher compared to the north-facing shoreline within Bay Jimmy (Fig. 7C). Previous studies have shown that the passage of cold fronts on the Gulf Coast increase suspended sediment in the water column (Roberts et al., 1987; Reed, 1989; Perez et al., 2000; Kineke et al., 2006), and in turn lead to large marsh accretion rates (Baumann, 1980; Reed, 1989; Cahoon et al., 1995). Because of the water level asymmetries this vertical accretion is not spatially uniform but instead depends on the orientation of the marsh. Waves impact the south-facing sites when water levels are above the marsh platform, and thus the sediment resuspended in front of the

marsh edge can deposit on the adjacent platform. Conversely, waves impact the north-facing sites when the water level is below the platform, thus preventing the sediment resuspended nearby to deposit on the platform.

The different elevation caused by the different accretion rates can then explain the difference in root shear strength between the north-facing and south-facing sites (Fig. 7B). Marsh plant species have strong zonation patterns related to the marsh elevation (Pennings and Callaway, 1992; Silvestri et al., 2005), and different species of marsh plants have different root structures that alter the soil erodibility and strength. For example, Wang et al. (2017) found that sediments with *Elytrigia artherica* roots had faster erosion rates in mesocosm experiments compared to *Spartina anglica*, *Aster tripolium*, and *Atriplex portulacoides*, and that erosion rates differed between each vegetation type. Similarly, tensile root strengths varied between several plant species of several plant species (*Spartina patens*, *Spartina alterniflora*, *Schoenoplectus americanus*, *Panicum hemitomon*, and *Sagittaria lancifolia*) in coastal Louisiana (Hollis and Turner, 2018). In addition, marshes with different elevations would have different soil drainage, which in turn could affect plant productivity. For example, an increased marsh elevation (of about

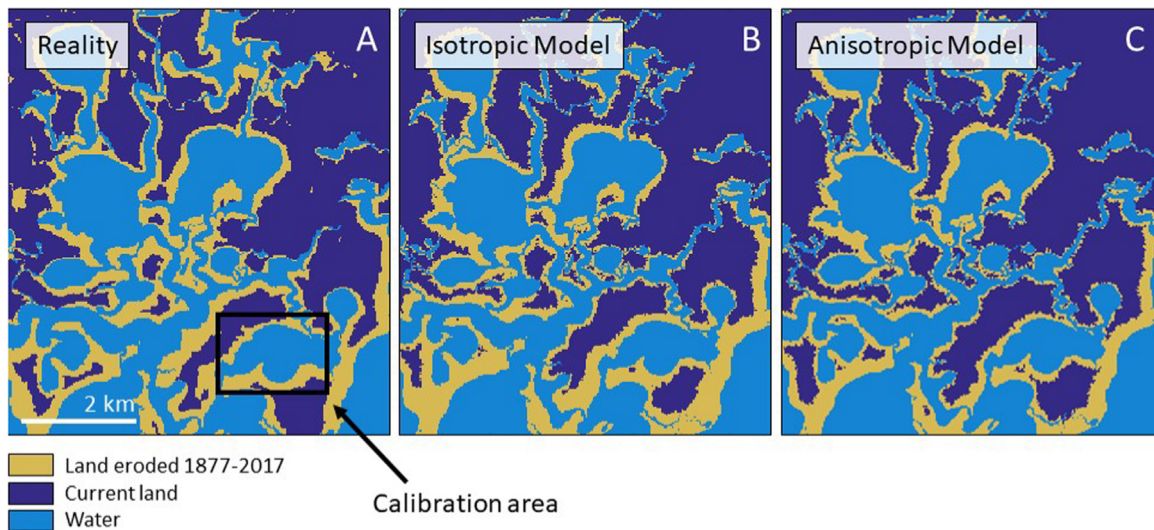


Fig. 8. (A) Actual land loss from 1877 to 2017 in Barataria Bay based on historical imagery. (B) Modeled land loss for same time period with isotropic model. (C) Modeled land loss for the same time period with anisotropic model. Yellow indicates land loss. Note the asymmetry of erosion on the north and south shores of the smaller bays in (A) and (C).

10 cm) has been associated with large changes in the belowground biomass of *S. alterniflora* in coastal Louisiana (Reed and Cahoon, 1992). Based on these observations, we would expect greater belowground biomass production and soil strength at the higher-elevation, south-facing site compared to the lower-elevation, north-facing site.

Furthermore, sediment composition and organic matter may also play an important role in the strength of the marsh. Previous studies have shown that grain size, bulk density, and organic matter content can be predictors in marsh erodibility (Feagin et al., 2009; Wang et al., 2017). The south-facing marshes also likely have a higher mineral content from aggradation during storm events, which further contributes to increasing marsh stability (Ravens et al., 2009). This

stronger soil would cause south-facing marshes to erode more slowly than north-facing marshes, thus partly explaining the observed asymmetry in erosion. Marsh soils in lower Barataria Bay are typically composed of silt and clays, have 20–35% organic matter, and have an average bulk density of 0.2–0.3 g cm⁻³ (Wilson and Allison, 2008; DeLaune and White, 2012; Pietroski et al., 2015). These values are consistent across studies within the lower basin, suggesting that most sites have similar basic soil properties. These properties were not measured at our study location, but appeared consistent with literature values. However, there could also be differences in these properties due to the differential accretion between north- and south-facing sites that further contribute to the differences in marsh strength.

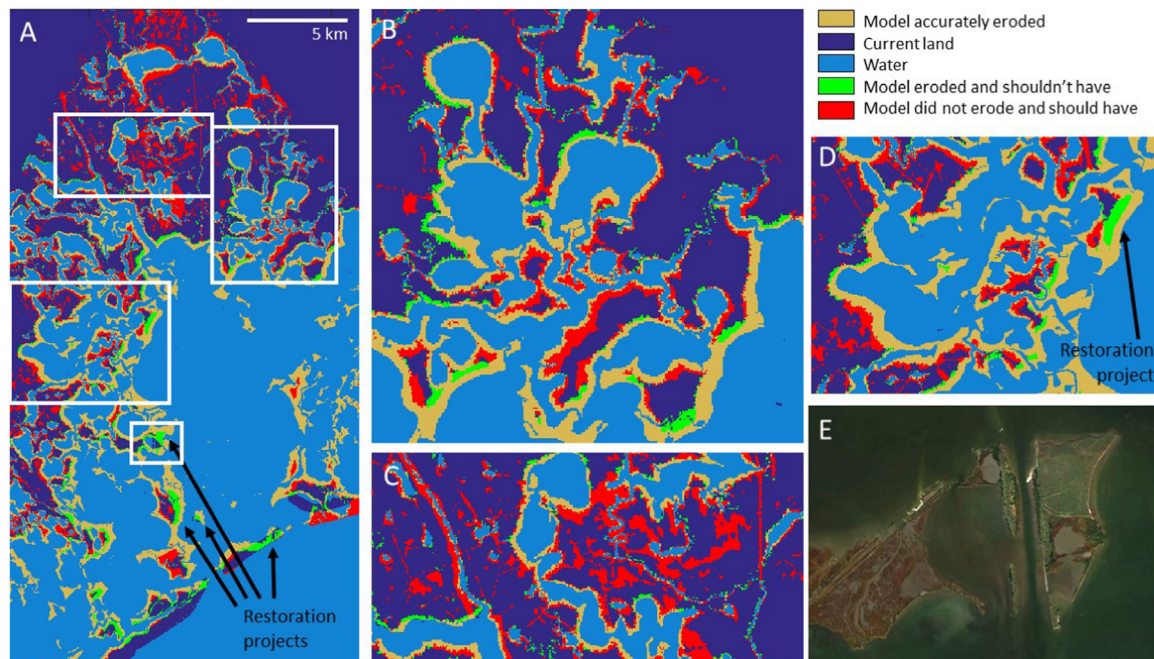


Fig. 9. Modeled land-loss results for 1877–2017 with wind-direction (anisotropic) correction. Yellow indicates land that was correctly eroded by the model, green indicates areas eroded by the model but not in reality, and red indicates areas that eroded in reality. (A) Entire model domain. (B) Some example of microbays that describe marsh edge erosion relatively well. (C) Areas of ponding which were not captured in the model. (D) Enclosed bays that were well-predicted by the model. The large green area in panel (D) is a site of marsh restoration; the model predicted this area would have eroded if action had not been taken. (E) Example of a restoration site that we were able to identify using the model.

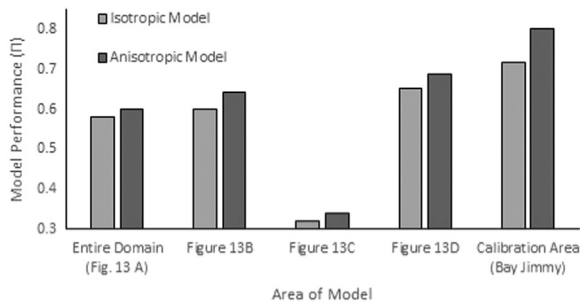


Fig. 10. Model performance (Π) for different regions of the model domain. Performance is calculated as in Eq. (5).

4.2. Model performance

We identified three processes that cause north-facing marsh edges to erode faster than south-facing edges: overshooting, undercutting, and spatial variability in marsh strength. Since all of these processes occur in unison throughout the bay, it is difficult to disentangle and determine the relative contribution of each process. Furthermore, there could be spatial variability in which process is dominant in a given region of Barataria Bay. Instead of implementing these processes directly in the model, we developed a single empirical correction, here referred to as effective erodibility (Eq. (5)), to account for all three processes.

The empirical correction applied to the erodibility coefficient in the marsh-edge erosion model was able to reproduce the observed asymmetry in Bay Jimmy and other microbays within Barataria Bay. The model performs best in small, semi-enclosed bays where the fetch is well-defined and the asymmetry of water levels and therefore erosion is most apparent (Figs. 8 and 11A–B, D). Wind-waves are the primary driver of erosion in these areas, as this is the only process incorporated into the model framework. The correction improves prediction of marsh edge erosion by 8% in Bay Jimmy ($\Pi = 0.72$ versus $\Pi = 0.80$), but only improves predictions of marsh edge erosion by 2% for the entire domain ($\Pi = 0.58$ versus $\Pi = 0.60$) (Fig. 10). While the improvement is slight over the whole domain, this is more indicative that some areas have more important controls on marsh loss than wind-wave erosion – namely, ponding, subsidence, and human effects. However, the entire basin is an area of active restoration projects and

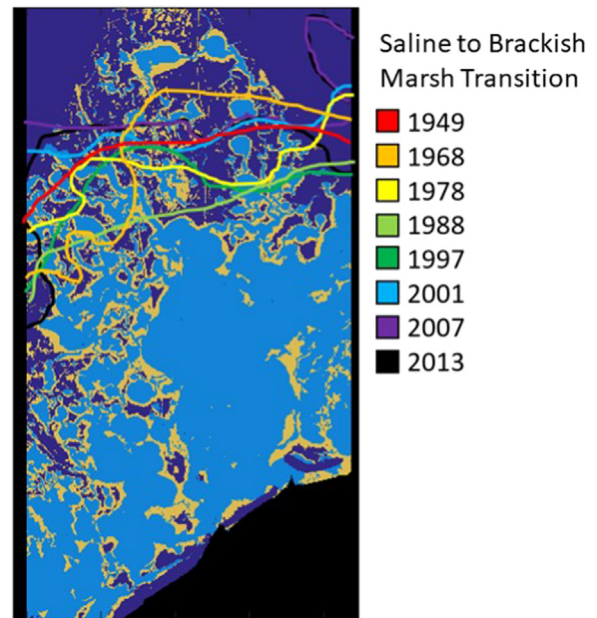


Fig. 12. Boundary of brackish and saline marsh over time overlain on map of actual erosion. Marsh survey data from the CRMS dataset.

experiences very high erosion rates, so small improvements in predictions could still be useful for planning purposes.

Several areas were not well-predicted by the model: the southern portion of the domain, near the barrier islands (Fig. 9A), and the upper portion of the domain, especially in the marsh interior (Fig. 9C). Near the barrier islands (Fig. 9A) the model did not perform well – both with and without the empirical correction – likely because the model does not incorporate barrier island processes that drive coastline change in these regions. The model under-predicted the amount of erosion in the marsh interior, particularly in northern Barataria Bay (Figs. 9C and 12). This mode of erosion is not due to wind-waves, but instead can be attributed to ponding and drowning of the marsh (Day et al., 2011; Mariotti, 2016; Ortiz et al., 2017). Interestingly, marsh survey data indicate that these regions have experienced both saline and brackish marsh conditions during the duration of the model run, which makes them more likely to experience die-back and ponding processes

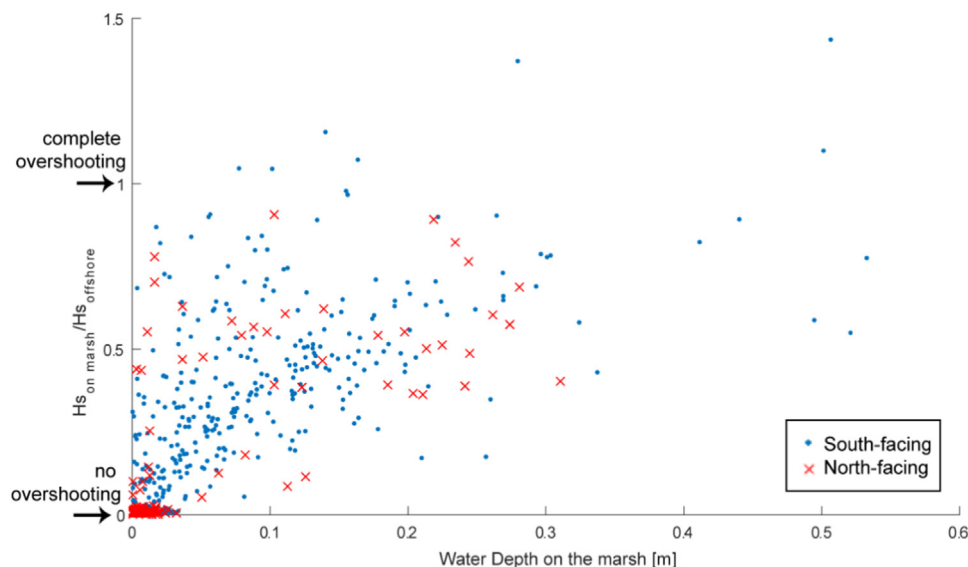


Fig. 11. Ratio of wave heights on marsh to wave heights in front of the marsh compared to water depth. A low value of the ratio indicates lower overshooting, and as the value approaches one, the amount of overshooting increases.

(Fig. 12). Furthermore, it is likely that the dominant plant species changed in these regions to reflect the salinity regime and this changed the rooting depth, belowground biomass, and other properties that influence soil strength and marsh erodibility.

Underpredictions of erosion by the model can also be explained by fault movement within Louisiana coastal basins, which cause localized subsidence and localized rapid marsh loss (Morton et al., 2002). Growth faults are common in Barataria Bay basin and have been active from the 1960s-present (Gagliano et al., 2003). Between 1964 and 1980, there was at least one major fault event along the Golden Meadow Fault zone, particularly on the Empire and Bastian Bay fault segments (both of which are in Barataria Basin), that resulted in a vertical offset ranging from centimeters to over a meter and a loss of 48–97 km² of marshes (Gagliano et al., 2003). The fault movement submerged these marshes, resulting in land loss that has no connection to wave action. For the model presented here, we excluded the southeast portion of Barataria Bay to omit the area that was most strongly impacted by this fault movement event. However, smaller fault movements continue throughout the basin and are expected to continue and are likely present in the model domain. These processes are not represented in the model and therefore are not captured in the results.

Likewise, areas of man-made modifications in the marsh, such as canals or restoration projects, are not represented in the model (Figs. 8A and 11E). Extensive modifications to Louisiana coastal lands have affected land loss, both directly and indirectly. For example, between 1900 and 2017 35,163 wells were permitted on land in coastal Louisiana parishes, resulting in an estimated 55,783 ha of canals dug out of coastal Louisiana lands (Turner and McClenachan, 2018) and therefore 55,783 ha of direct land loss. Additionally, upstream reaches of the Mississippi river were dammed in the 1950s, reducing sediment supply, leading to indirect land loss (Kesel, 1989). This was further exacerbated by levee construction starting in the late 1920s, which eliminated the connection between the river and the marshlands, which also resulted in indirect land loss (Kesel, 1989). Additionally, there have been numerous restoration projects including marsh creation, beach nourishment, and breakwaters across the Louisiana coast for at least the last 100 years (CPRA, 2017). The land changes associated with these human activities certainly affects the accuracy of a model that does not incorporate these processes.

Noticeably, the modeled false positives (areas of overpredicted erosion) tend to overlap with areas of marsh restoration projects (Fig. 9A, E), which are particularly numerous in Barataria Bay. These projects, ranging from ~8 km² to almost 35 km², generally consist of an armoring of the marsh edge or the construction of a new ridge that is then backfilled with dredged sediments (CPRA, 2017). Because the model does not include these anthropogenic effects, these areas are predicted to erode as if the marsh was unaltered. Therefore, the size of the erosion overprediction can be used to estimate the amount of marsh loss prevented by a specific restoration projects (examples in Fig. 9A, E).

The model accurately predicted coastline changes even though it did not directly include any effects from oil spills such as that from the Deepwater Horizons. A possible explanation is that, despite marsh oiling temporarily increasing both interior and edge erosion rates (McClenachan et al., 2013; Ragoonwala et al., 2016), its effect vanishes after 3–6 years (Beland et al., 2017). Given that large marsh oilings are infrequent, their long-term effects are likely small compared to the other processes contributing to marsh edge erosion. This small contribution from oiling was indirectly accounted for in the model through the calibrated background erodibility coefficient, α_0 . Thus, although oiling might create hotspots of marsh edge erosion at a yearly to decadal time scale, its effects are not crucial in predicting spatial patterns of marsh edge erosion at the multi-decadal to centennial time scales simulated in our model.

4.3. Applications outside of Barataria Bay

The model focused on creating a computationally-efficient way to include the effect of wind-induced water level changes on marsh edge erodibility. Water level change due to winds is not unusual or restricted to Barataria Bay. For example, many microtidal bays along the Gulf coast of the United States – including Terrebonne, Mobile, and Galveston Bay – are likely to have similar relationships between water level and wind. For example, a study showed that water levels in Galveston Bay were correlated with easterly and westerly winds (Blaha and Sturges, 1981). Because marsh characteristics and tidal range are similar along the US Gulf Coast, it is plausible to assume that water levels might affect marsh erosion similarly to what we observed in Barataria Bay, and thus the model could be applied to these systems.

Despite that using wind direction as a proxy for marsh erodibility is effective for Barataria Bay – and possibly other sites along the Gulf Coast of the United States – this method may not be applicable to other locations. A more general method would require one to 1) directly simulate water levels in space and time, and 2) directly implement the effect that water level has on the three processes described in this study (overshooting, undercutting, erodibility variations). Both steps would require more sophisticated modeling and data integration, an effort that might be justified where short-term and location-specific predictions are needed.

In systems where water level asymmetries and spatial heterogeneities are either absent or not known a priori, the standard marsh edge erosion model (i.e., with a constant value for the erodibility coefficient α) should be applied. In this case, any variability in the rate of marsh edge retreat would be associated with the wind distribution and the bay geometry (i.e., the spatial distribution of the fetch). This simpler approach could provide first-order estimates, and could lead to the formulation of further hypotheses regarding mechanisms of marsh erosion.

4.4. Extreme events

Hurricanes and other extreme events are associated with drastic changes to coastal systems. Ragoonwala et al. (2016) showed that hurricane Isaac increased erosion rates in Barataria Bay by a factor of 2–3 mainly due to wind-wave attack of exposed shorelines. The effect of extreme events is automatically included in the model, which randomly selects wind speeds from the 28-year time series at Southwest Pass (Fig. 1). For the strongest wind speed on record (29 ms⁻¹), the calculated wave power in Bay Jimmy is 245.4 Wm⁻¹, resulting in an instantaneous erosion rate of 77 m yr⁻¹.

Despite the rapid erosion rate, the rarity and short duration of extreme events makes them less important in the long-term dynamics of marsh edge erosion. Indeed, the largest amount of erosion was associated with a wave power of 7.4 Wm⁻¹, which relates to a wind speed of 5.8 ms⁻¹ (Fig. 13). This is consistent with a previous finding that moderate winds, and therefore moderate waves, are the most important in marsh edge erosion (Leonardi et al., 2016).

Other processes that were not included in the model may become more important during hurricanes. For example, hurricanes create storm surges, which change the dynamics at the marsh edge. The water level would be high compared to the marsh edge and exert less wave thrust on the edge (Tonelli et al., 2010), potentially decreasing the overall effect of hurricanes on the marsh edge. However, other mechanisms of erosion, such as the mass removal of marsh plants from the marsh platform (“marshballs”), may become more important and drive geomorphic change (Day et al., 2007; Howes et al., 2010). The formation of marshballs, along with other mechanisms of erosion that might be more common during extreme events, are not included in our model and can account for some of the discrepancies, particularly in the marsh interior.

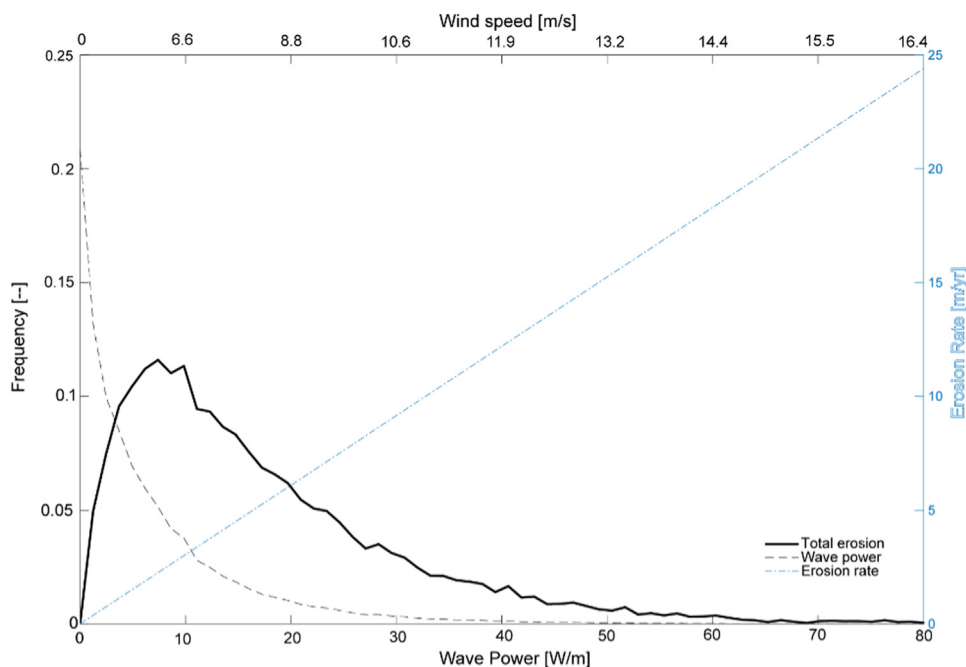


Fig. 13. Frequency-magnitude distribution of wave power (dashed back line), total erosion (black line), and erosion rate (dash-dot blue line) as a function of wave power. Wind speeds corresponding to the wave power are on the upper x-axis. Calculations are based on Bay Jimmy (depth: 0.8 m, fetch: 1.5 km, erodibility coefficient: $0.312 \text{ (m yr}^{-1})/(\text{W m}^{-1})$).

4.5. Policy implications

This study demonstrates that, depending on the orientation of the marsh shoreline (north- or south-facing), different layers of the marsh edge are more vulnerable to wave impact; south-facing shores are more vulnerable near the top of the marsh platform whereas north-facing shores are more vulnerable at the base of the marsh edge. This result can be used to inform projects aimed to protect the marsh edge. For example, protection of south-facing marsh edges should focus on the vegetated portion, whereas protection of north-facing marsh shores should focus on stabilizing the toe of the marsh edge. The false negatives of the model (areas of erosion underprediction) can also be a useful tool in determining which processes are not associated with wave erosion, and can thus help identify the most effective restoration or protection project.

In a future with no action, the Louisiana coast expects to lose \$3.6 billion in infrastructure replacement over the next 50 years – an infrastructure that supports an additional \$7.6 billion of economic activity across the United States each year (Barnes and Virgets, 2017). To mitigate this, the Louisiana Coastal Master Plan was developed to decrease land loss and protect infrastructure by investing \$50 billion over 50 years in coastal Louisiana protection and restoration projects. Between 1990 and 2013, more than 150 restoration projects had been funded, costing more than a billion dollars (Peyronnin et al., 2013). Despite the fact that restoration projects are being implemented, there are a limited number of studies assessing their success, particularly in a quantitative way (Wortley et al., 2013; Suding, 2011). The results of our model can provide a quantitative assessment of land change, or lack thereof, as a result of specific restoration projects, and can thus be used in cost-benefit analysis for the socioeconomic and ecologic value of restoration projects.

5. Conclusions

Wind patterns in coastal Louisiana drive large water level changes that affect the rates of marsh edge erosion. We identified three wind-related processes that could affect marsh edge erosion: overshooting, undercutting, and spatial variations in marsh strength. Southerly winds increase the water level in the bay causing waves to overshoot the marsh platform, limiting their effect on edge erosion. Northerly winds

decrease the water level, causing waves to impact the lower, more erodible layers of the marsh edge. Northerly and southerly winds also lead to differences in marsh elevation at the marsh edge, resulting in different marsh strengths, which we attributed to differences in plant communities and root strength. These three processes collectively increase the erosion rates at north-facing marsh shorelines compared to south-facing ones.

Using a simple empirical correction that encompasses these processes, we made more accurate predictions of marsh edge erosion on the decadal to centennial time-scale, which is of most relevance to coastal communities and policy makers. The model false negatives can be used to identify mechanisms of marsh loss not associated with wave erosion, whereas the model false positives can be used to quantify the marsh loss prevented by specific marsh protection projects. Wind patterns and their effects on water level in microtidal coastal bays should be considered in marsh edge erosion models and predictions, not only in Louisiana, but other environments where wind patterns impact water levels.

Acknowledgements

We thank J. Robinson, S. Murshid, N. Rabalais, S. Taylor, T. Quirk, M. Kelsall, A. Bonisoli-Alquati, A. Perez-Umphrey, and A. Cole for help with field work and support on this project. We also would like to thank the editor, an anonymous reviewer, and I. Georgiou for comments on this manuscript that greatly improved the quality and clarity. KV was funded by a Louisiana Board of Regents fellowship. This research was made possible by a grant from the Gulf of Mexico Research Initiative. Data are publicly available through the Gulf of Mexico Research Initiative Information and Data Cooperative (GRIIDC) at <https://data.gulfresearchinitiative.org> (doi: 10.7266/N72V2DMF).

References

- Barnes, S.R., Virgets, S., 2017. Regional Impacts of Coastal Land Loss and Louisiana's Opportunity for Growth. LSU EJ Ourso College of Business Economics and Policy Research Group, Environmental Defense Fund.
- Baumann, R.H., 1980. Mechanisms of Maintaining Marsh Elevation in a Subsiding Environment (M. Sc. Thesis). Louisiana State University, Baton Rouge, Louisiana.
- Beland, M., Biggs, T.W., Roberts, D.A., Peterson, S.H., 2017. Oiling accelerates loss of salt marshes, southeastern Louisiana. *PLoS One* 12 (8), e0181197.
- Bendoni, M., Mel, R., Solari, L., Lanzoni, S., Francalanci, S., Oumeraci, H., 2016. Insights

- into lateral marsh retreat mechanism through localized field measurements. *Water Resour. Res.* 52 (2), 1446–1464.
- Bertness, M.D., 1984. Ribbed mussels and *Spartina alterniflora* production in a New England salt marsh. *Ecology* 65, 1794–1807.
- Blaha, J., Sturges, W., 1981. Evidence for wind-forced circulation in the Gulf of Mexico. *J. Mar. Res.* 39, 711–734.
- Cahoon, D., Reed, D., Day, J., Steyer, G., Boutmans, R., Lynch, J., McNally, D., Latif, N., 1995. The influence of Hurricane Andrew on sediment distribution in Louisiana coastal marshes. *J. Coast. Res.* 18, 280–294.
- Chen, Y., Thompson, C.E.L., Collins, M.B., 2012. Saltmarsh creek bank stability: biostabilisation and consolidation with depth. *Cont. Shelf Res.* 35, 64–74.
- Coastal Protection and Restoration Authority of Louisiana (CPRA), 2017. Louisiana's Comprehensive Master Plan for a Sustainable Coast. Coastal Protection and Restoration Authority of Louisiana, Baton Rouge, LA.
- Couvillion, B.R., Barras, J.A., Steyer, G.D., Sleavin, W., Fischer, M., Beck, H., Trahan, N., Griffin, B., Heckman, D., 2011. Land area change in coastal Louisiana from 1932 to 2010: U.S. Geological Survey Scientific Investigations Map 3164, scale 1:265,000, 12 p. pamphlet.
- Couvillion, B.R., Beck, H., Schoolmaster, D., Fischer, M., 2017. Land area change in coastal Louisiana 1932 to 2016: US Geological Survey Scientific Investigations Map 3381, 16 p. pamphlet.
- Day, J.W., Boesch, D.F., Clairain, E.J., Kemp, G.P., Laska, S.B., Mitsch, W.J., Orth, R., Mashriqui, H., Reed, D.J., Shabman, L., Simentad, C.A., Streever, B.J., Twilley, R.R., Watson, C.C., Wells, J.T., Whigham, D.F., 2007. Restoration of the Mississippi Delta: lessons from Hurricanes Katrina and Rita. *Science* 315, 1679–1684.
- Day, J.W., Kemp, G.P., Reed, D.J., Cahoon, D.R., Boumans, R.M., Suhayda, J.M., Gambrell, R., 2011. Vegetation death and rapid loss of surface elevation in two contrasting Mississippi delta salt marshes: the role of sedimentation, autocompaction, and sea-level rise. *Ecol. Eng.* 37 (2), 229–240.
- DeLaune, R.D., White, J.R., 2012. Will coastal wetlands continue to sequester carbon in response to an increase in global sea level? a case study of the rapidly subsiding Mississippi river deltaic plain. *Clim. Change* 110, 297–314.
- Dimego, G.J., Bosart, L.F., Endersen, G.W., 1976. An examination of the frequency and mean conditions surrounding frontal incursions into the Gulf of Mexico and Caribbean Sea. *Mon. Weather Rev.* 104, 709–718.
- Ensign, S., Currin, C., Piehler, M., Tobias, C., 2017. A method for using shoreline morphology to predict suspended sediment concentration in tidal creeks. *Geomorphology* 276, 280–288.
- Escapa, M., Minkoff, D.R., Perillo, G.M.E., Iribarne, O., 2007. Direct and indirect effects of burrowing crab *Chasmagnathus granulatus*: erosion of southwest Atlantic *Sarcocornia*-dominated marshes. *Limnol. Oceanogr.* 52 (6), 2340–2349.
- Fagherazzi, S., Wiberg, P.L., 2009. Importance of wind conditions, fetch, and water levels on wave-generated shear stresses in shallow intertidal basins. *J. Geophys. Res.* 114, F03022.
- Feagin, R.A., Lozada-Bernard, S.M., Ravens, T.M., Moller, I., Yeager, K.M., Baird, A.H., 2009. Does vegetation prevent wave erosion of salt marsh edges? *PNAS* 106 (25), 10109–10113.
- Feng, Z., Li, C., 2010. Cold-front-induced flushing of the Louisiana Bays. *J. Mar. Syst.* 82 (4), 252–264.
- Francalanci, S., Bendoni, M., Rinaldi, M., Solari, L., 2013. Ecomorphodynamic evolution of salt marshes: experimental observation of bank retreat processes. *Geomorphology* 195, 53–65.
- Gabet, E.J., 1998. Lateral migration and bank erosion in a saltmarsh tidal channel in San Francisco Bay, California. *Estuaries* 21, 745–753.
- Gagliano, S.M., Kemp, E.B., Wicker, K.M., Wiltenthuth, K.S., 2003. Active geological faults and land change in southeastern Louisiana. *Study U.S. Army Corps Eng.* 204.
- Hartig, E.K., Gornitz, V., Kolker, A., Muschacke, F., Fallon, D., 2002. Anthropogenic and climate-change impacts on salt marshes of Jamaica Bay, New York City. *Wetlands* 22, 71–89.
- Hollis, L.O., Turner, R.E., 2018. The tensile root strength of five emergent coastal macrophytes. *Aquat. Bot.* 146, 39–47.
- Howes, N.C., FitzGerald, D.M., Hughes, Z.J., Georgiou, I.Y., Kulp, M.A., Miner, M.D., Smith, J.M., Barras, J.A., 2010. Hurricane-induced failure of low salinity wetlands. *PNAS* 107 (32), 14014–14019.
- Hsu, S.A., 1988. Coastal Meteorology. Academic Press, San Diego, California (260 pp).
- Hughes, Z.J., FitzGerald, D.M., Wilson, C.A., Pennings, S.C., Wieske, K., Mahadevan, A., 2009. Rapid headward erosion of marsh creeks in response to relative sea level rise. *Geophys. Res. Lett.* 36 (3).
- Kemp, G.P., Wells, J.T., Van Heerden, I.L., 1980. Frontal passages affect delta development in Louisiana. *Coast. Oceanogr. Climatol. News* 3, 4–5.
- Kesel, R.H., 1989. The role of the Mississippi River in wetland loss in southeastern Louisiana, USA. *Environ. Geol. Water Sci.* 13 (3), 183–193.
- Kineke, G.C., Higgins, E.E., Hart, K., Velasco, D., 2006. Fine-sediment transport association with cold-front passages on the shallow shelf, Gulf of Mexico. *Cont. Shelf Res.* 26 (17–18), 2073–2091.
- Kolker, A.S., Allison, M.A., Hameed, S., 2011. An evaluation of subsidence rates and sea-level variability in the northern Gulf of Mexico. *Geophys. Res. Lett.* 38, L21404. <https://doi.org/10.1029/2011GL049458>.
- Le Hir, P., Monbet, Y., Orvain, F., 2007. Sediment erodibility in sediment transport modelling: can we account for biota effects? *Cont. Shelf Res.* 27 (8), 1116–1142.
- Leonardi, N., Fagherazzi, S., 2014. How waves shape salt marshes. *Geology* 42 (10), 887–890.
- Leonardi, N., Ganju, N.K., Fagherazzi, S., 2016. A linear relationship between wave power and erosion determines salt-marsh resilience to violent storms and hurricanes. *PNAS* 113 (1), 64–68.
- Marani, M., d'Alpaos, A., Lanzoni, S., Santalucia, M., 2011. Understanding and predicting wave erosion of marsh edges. *GRL* 38 (21).
- Mariotti, G., 2018. Marsh channel morphological response to sea level rise and sediment supply. *Estuar. Coast. Shelf Sci.* 209, 89–101.
- Mariotti, G., 2016. Revisiting salt marsh resilience to sea level rise: are ponds responsible for permanent land loss? *JGR: Earth Surf.* 121 (7), 1391–1407.
- Mariotti, G., Huang, H., Xue, Z., Li, B., Justic, D., Zang, Z., 2018. Biased wind measurements in estuarine waters. *JGR: Oceans* 123 (3577:3587).
- Mariotti, G., Canestrelli, A., 2017. Long-term morphodynamics of muddy backbarrier basins: fill in or empty out? *Water Resour. Res.*
- Mariotti, G., Kearney, W.S., Fagherazzi, S., 2016. Soil creep in salt marshes. *Geology* 44 (6), 459–462.
- Mariotti, G., Fagherazzi, S., 2010. A numerical model for the coupled long-term evolution of salt marshes and tidal flats. *JGR: Earth Surf.* 115 (F1).
- Mariotti, G., Fagherazzi, S., Wiberg, P.L., McGlathery, K.J., Carniello, L., Defina, A., 2010. Influence of storm surges and sea level on shallow tidal basin erosive processes. *J. Geophys. Res.* 115, C11012.
- McClenachan, G., Turner, R.E., Tweel, A.W., 2013. Effects of oil on the rate and trajectory of Louisiana marsh shoreline erosion. *Environ. Res. Lett.* 8, 044030.
- McLoughlin, S.M., 2010. Erosional Processes Along Salt Marsh Edges on the Eastern Shore of Virginia (MS Thesis). University of Virginia, Charlottesville, VA.
- Moller, I., Kudella, M., Rupprecht, F., Spencer, T., Paul, M., van Wesenbeeck, B.K., Wolters, G., Jensen, K., Bouma, T.J., Miranda-Lange, M., Schimmels, S., 2014. Wave attenuation over coastal salt marshes under storm surge conditions. *Nat. Geosci.* 7, 727–731.
- Moller, I., Spencer, T., 2002. Wave dissipation over macro-tidal saltmarshes: effects of marsh edge typology and vegetation change. *J. Coast. Res.* SI36, 506–521.
- Morton, R.A., Buster, N.A., Krohn, M.D., 2002. Subsurface controls on historical subsidence rates and associated wetland loss in southcentral Louisiana. *Trans. Gulf Coast Assoc. Geol. Soc.* 52, 767–778.
- Murray, S.P., 1976. Currents and circulation in the coastal waters of Louisiana, Center for Wetland Resources, Louisiana State University, Sea Grant publication number LSU-T-76-003.
- Nixon, Z., Zengel, S., Baker, M., Steinhoff, M., Fricano, G., Rouhani, S., Michel, J., 2016. Shoreline oiling from the Deepwater Horizon oil spill. *Mar. Pollut. Bull.* 107 (1), 170–178.
- Olea, R.A., Coleman, J.L., 2014. A synoptic examination of causes of land loss in southern Louisiana as related to the exploitation of subsurface geological resources. *J. Coast. Res.* 30 (5), 1025–1044.
- Ortiz, A.C., Roy, S., Edmonds, D.A., 2017. Land loss by pond expansion on the Mississippi River Delta plain. *GRL* 44 (8), 3635–3642.
- Pennings, S.C., Callaway, R.M., 1992. Salt marsh plant zonation: the relative importance of competition and physical factors. *Ecology* 73 (2), 681–690.
- Perez, B.C., Day, J.W., Rouse, L.J., Shaw, R.F., Wang, M., 2000. Influence of Atchafalaya river discharge and winter frontal passage on suspended sediment concentration and flux in Fourleague Bay, Louisiana. *Estuar. Coast. Shelf Sci.* 50, 271–290.
- Peyronnin, N., Green, M., Richards, C.P., Owens, A., Reed, D., Chamberlain, J., Groves, D.G., Rhinehart, W.K., Belhadjali, K., 2013. Louisiana's 2012 Coastal Master Plan: overview of a science-based and publicly informed decision-making process. *J. Coast. Res.* SI 67, 1–15.
- Pietroski, J.P., White, J.R., DeLaune, R.D., 2015. Effects of dispersant used for oil spill remediation on nitrogen cycling in Louisiana coastal salt marsh soil. *Chemosphere* 119, 562–567.
- Prietas, A.M., Mariotti, G., Leonardi, N., Fagherazzi, S., 2015. Coupled wave energy and erosion dynamics along a salt marsh boundary, Hog Island Bay, Virginia, USA. *J. Mar. Sci. Eng.* 3, 1041–1065.
- Rangoonwala, A., Jones, C.E., Ramsey, E., 2016. Wetland shoreline recession in the Mississippi River Delta from petroleum oiling and cyclonic storms. *Geophys. Res. Lett.* 43 (22), 11652–11660.
- Raposa, K.B., McKinney, R.A., Wigand, C., Hollister, J.W., Lovall, C., Szura, K., Gurak, J.A., McNamee, J., Raithe, C., Watson, E.B., 2018. Top-down and bottom-up controls on southern New England salt marsh crab populations. *PeerJ* 6, e4876. <https://doi.org/10.7717/peerj.4876>.
- Ravens, T.M., Thomas, R.C., Roberts, K.A., Santschi, P.H., 2009. Causes of salt marsh erosion in Galveston Bay, Texas. *J. Coast. Res.* 25, 265–272.
- Reed, D.J., 1989. Patters of sediment deposition in subsiding coastal salt marshes, Terrebonne Bay, Louisiana: the role of winter storms. *Estuaries* 12 (4), 222–227.
- Reed, D.J., Cahoon, D.R., 1992. The relationship between marsh surface topography, hydroperiod, and growth of *Spartina alterniflora* in a deteriorating Louisiana salt marsh. *J. Coast. Res.* 8 (1), 77–87.
- Roberts, H.H., Huh, O.K., Hsu, S.A., Rouse, L.J., Rickman, D., 1987. Impact of cold-front passages on geomorphic evolution and sediment dynamics of the complex Louisiana coast. *Coast. Sediment. 1950–1963 (ASCE)*.
- Schepers, L., 2017. Spatial Patterns and Bio-geomorphological Effects of Vegetation Loss in a Submerging Coastal Marsh (Dissertation). University of Antwerp.
- Schwimmer, R.A., 2001. Rates and processes of marsh shoreline erosion in Rehoboth Bay, Delaware, USA. *J. Coast. Res.* 17 (3), 672–683.
- Silvestri, S., Defina, A., Marani, M., 2005. Tidal regime, salinity and salt marsh plant zonation. *Estuar. Coast. Shelf Sci.* 62 (1–2), 119–130.
- Smith, S.M., 2009. Multi-decadal changes in salt marshes of Cape cod, MA: photographic analyses of vegetation loss, species shifts, and geomorphic change. *Northeast. Nat.* 16, 183–208. <https://doi.org/10.1656/045.016.0203>.
- Suding, K.N., 2011. Toward an era of restoration in ecology: successes, failures, and opportunities ahead. *Annu. Rev. Ecol. Evol. Syst.* 42, 465–487.
- Tonelli, M., Fagherazzi, S., Petti, M., 2010. Modeling wave impact on salt marsh boundaries. *J. Geophys. Res.* 115, C09028.
- Tucker, M.J., Pitt, E.G., 2001. Waves in ocean engineering, No. volume 5.

- Turner, R.E., McClenachan, G., 2018. Reversing wetland death from 35,000 cuts: opportunities to restore Louisiana's dredged canals. *PLoS One* 13 (12), e0207717.
- Turner, R.E., 2014. A synoptic examination of causes of land loss in southern Louisiana as related to the exploitation of subsurface geological resources (Discussion of: Olea, R.A., and Coleman, J.L., Jr., 2014). *J. Coast. Res.* 30 (5), 1025–1044 (*Journal of Coastal Research* 30)(6): 1330–1334).
- Turner, R.E., 2011. Beneath the salt marsh canopy: loss of soil strength with increasing nutrient loads. *Estuaries Coasts* 34 (5), 1084–1093.
- Wang, H., van der Wal, D., Li, X., van Belzen, J., Herman, P.M.J., Hu, Z., Ge, Z., Zhang, L., Bouma, T.J., 2017. Zooming in and out: scale dependence of extrinsic and intrinsic factors affecting salt marsh erosion. *JGR: Earth Surf.* 122, 1455–1470.
- Wax, C.L., 1977. An Analysis of the Relationship Between Water Level Fluctuations and Climate, Coastal Louisiana (Ph.D. Dissertation). Louisiana State University.
- Wilson, C., Allison, M., 2008. An equilibrium profile model for retreating marsh shorelines in southeast Louisiana. *Estuar. Coast. Shelf Sci.* 80, 483–494.
- Wortley, L., Hero, J.-M., Howes, M., 2013. Evaluating ecological restoration success: a review of the literature. *Restor. Ecol.* 21 (5), 537–543.
- Young, I.R., Verhagen, L.A., 1996. The growth of fetch limited waves in water of finite depth. Part 1. total energy and peak frequency. *Coast. Eng.* 29 (1–2), 47–78.